Static and dynamical properties of elliptical quantum corrals

M. Nizama,[1] K. Hallberg,[1] and J. d'Albuquerque e Castro[2]

[1]*Centro Atómico Bariloche and Instituto Balseiro, Comisión Nacional de Energía Atómica, 8400 Bariloche, Argentina*
[2]*Instituto de Fisica, Universidade Federal do Rio de Janeiro, CEP 21941-901 Rio de Janeiro, Brazil*
(Received 28 December 2006; revised manuscript received 19 April 2007; published 27 June 2007)

Due to their focalizing properties, elliptic quantum corrals present very interesting physical behaviors. In this work, we analyze static and dynamical properties of these systems. Results are presented for realistic values of the parameters, which might be useful for comparison with experiments. We study noninteracting corrals and their response to several kinds of external perturbations, observing that, for realistic values of the Fermi level, the dynamics involves only a few number of excited states, making the system quite robust with respect to possible sources of decoherence. We also study the system in the presence of two $S=1/2$ impurities located at its foci, which interact with the electrons of the ellipse via a superexchange interaction J. This system is diagonalized numerically and properties such as the spin gap and spin-spin static and dynamical correlations are studied. We find that, for small J, both spins are locked in a singlet or triplet state, for even or odd filling, respectively, and its spin dynamics consists mainly of a single peak above the spin gap. In this limit, we can define an effective Heisenberg Hamiltonian to describe the low-energy properties. For larger J, more states are involved and the localized spins decorrelate in a manner similar to the Ruderman-Kittel-Kasuya-Yosida-Kondo transition for the two-impurity problem.

I. INTRODUCTION

The recent advancement in the knowledge and fabrication techniques of nanoscopic systems has revealed a great variety of novel physical behaviors, a striking example of which is the observation of the phenomenon now known as the *quantum mirage*.[1] This effect arises in nanoscopic systems called quantum corrals, where the electron wave functions are confined to a finite region by means of a barrier formed by atoms encircling a closed region in space.

Quantum corrals are built by positioning atoms, typically transition metal atoms, along a closed line on the clean surfaces of noble metals. In their recent experiments, Manoharan *et al.*[1] have built elliptical corrals with Co atoms on the (111) plane of Cu. The Cu (111) surface has a band of surface states, orthogonal to the bulk states, which can be represented as a confined two dimensional electron gas. The Fermi level is placed at 450 meV above the bottom of the surface state band. The atoms forming the corral act as scattering centers which tend to confine the surface electrons inside the corral.

A number of theoretical papers analyzed these experiments, with one or more impurities considering different configurations[2–10] (see also complete review articles in Refs. 12 and 13). In Refs. 9 and 10, it was suggested that, as a consequence of the focalizing properties of quantum elliptical corrals, two impurities located at the foci of the system will strongly interact. Such a prediction has been supported by Stepanyuk *et al.*,[11] who reported results of first principles calculations of the exchange coupling between magnetic impurities inside quantum corrals.

The physical properties of quantum corrals are affected by several factors, which include confinement, quantum interference, and many-body effects. So far, interest has been focused on the static properties of quantum corrals, leaving the dynamical behavior of such systems almost unexplored.

In this work, we have studied static and dynamical physical properties of elliptical quantum corrals for various models and perturbations, where the focalizing properties of the system have important consequences in the physical behavior.

We have considered two cases. The first one consisted of an isolated ellipse describing a closed quantum system containing an arbitrary number of noninteracting electrons up to a certain Fermi energy. The system was perturbed by either local potentials located on the foci of the ellipse or a potential in the form of a barrier cutting the ellipse through its minor axis. In the second case, two impurity spins interacting via a superexchange term with the electrons in the ellipse were added to the foci of the system. This many-body problem was treated numerically, and static properties, like the spin gap, and dynamical responses, including real-time behavior, were analyzed.

II. NONINTERACTING CASE

Throughout this work we have adopted a simplified description of the system, based on a spinless tight-binding model defined on a discretized square lattice within the boundaries of the ellipse, with eccentricity $\epsilon=0.6$ and hopping element t^* between nearest neighbors. The Hamiltonian in this case is simple and reads $H_{el}=-t^*\Sigma_{\langle i,j\rangle}c_i^\dagger c_j$, where the sites i and j run inside the ellipse which consists of around 1000 sites or atoms. Here, we have considered a constant zero local energy in each site. As we will be analyzing low-energy wave functions with wavelengths much larger than the real interatomic distance, the underlying atomic distribution is irrelevant.[13] Our calculations could have also relied on the exact solutions for a continuum ellipse (Mathieu functions).

The Fermi energy was set to coincide with its 23rd eigenstate $|\psi_{23}\rangle$, which is similar to the state at the Fermi energy in
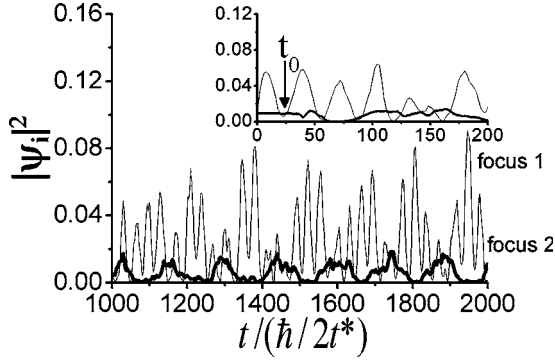
FIG. 1. Time dependence of the probability density in both foci for a negative potential, $V_1=-1$, applied in focus 1 at time $t=0$. Insets depict short times, and t_0 is the time elapsed until the perturbation reaches the unperturbed focus. For $t^*=1$ eV, typical periods in this figure are around 5×10^{-14} s.

the experimental setup of Ref. 1 [see Fig. 5(a)]. This configuration is not crucial for the main conclusions, and other eccentricities and reference levels will have a similar behavior, as long as the wave function bears an appreciable weight at the foci of the ellipse.

We have studied the time evolution of the wave function at the Fermi energy when, at time $t=0$, a constant negative or positive potential V_1 is applied to focus 1: $\exp(-iHt)|\psi_{23}\rangle$, where $H=H_{el}+V_1(t)$. Figures 1–3 show the square of the amplitude of such a wave function in foci 1 and 2 for $t\geq0$, for three distinct cases corresponding to $V_1=-1$ (Fig. 1), $V_1=1$ (Fig. 2), and $V_1=V_2=-1$ (Fig. 3). We notice that, in the two first figures, a finite time t_0 elapses between the onset of the perturbation in focus 1 and the observation of the response in focus 2, as shown in the insets, which is of the order of $t_0 \sim 20\hbar/2t^* \sim 10^{-14}$ s, where we have used $t^*=1$ eV (see below).

Another interesting point regards the oscillatory behavior of the two squared amplitudes for $t>t_0$. The occurrence of oscillations in the probability amplitude in the presence of a time-independent potential (for $t>0$) as well as the overall "seesaw" or alternating behavior between both foci, i.e., when the probability is high in one focus, it is low in the other, and vice versa (except for the higher order oscillations in focus 1 for negative V_1), are intimately related to quantum interference effects within the ellipse. The period of these oscillations is of the order of the energy difference corre-
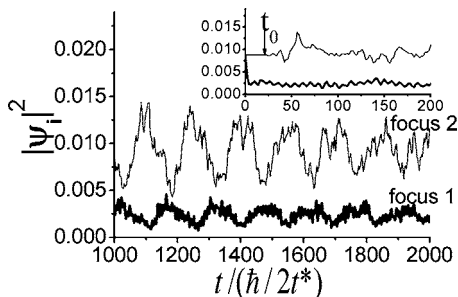

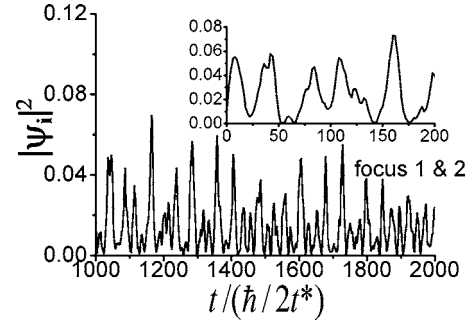FIG. 2. Same as Fig. 1 but for a positive potential in focus 1, $V_1=1$.

FIG. 3. Same as Fig. 1 but for a symmetric negative potential applied to foci 1 and 2, $V_1=V_2=-1$.

sponding to the main transitions involved, i.e., states 18, 23, and 29 for this configuration. Using the parameters of Refs. 1, 3, and 4 for the case of the ellipse on the copper [111] surface, i.e., distance between foci $d=70$ Å, total ellipse area of 85.7 nm^2, and $t^*=1$ eV, we obtain periods of the order of $h/(E_{23}-E_{18})\simeq5\times10^{-14}$ s, where $E_{23}-E_{18}=0.0754t^* =75$ meV (the transition between states 23 and 29 has a similar value). We remark that this energy is 1–2 orders of magnitude larger than the Kondo temperature in quantum dots. An animated version of these behaviors is found in Ref. 14. We notice that the amplitude of oscillation in focus 1 is larger than that in focus 2 when V_1 is negative (attractive potential, Fig. 1), and smaller when V_1 is positive (repulsive potential, Fig. 2).

As a matter of corroboration, using the above set of parameters, we obtain for the Fermi velocity of the electrons involved in the transmission of the information from one focus to the other the value $v_F=d/t_0=0.8\times10^8$ cm/s (where we have considered the focal distance $d\simeq70\times10^{-8}$ cm and $t_0\simeq0.87\times10^{-14}$ s), which is of the same order of magnitude as the one calculated in Ref. 3.

We have also calculated the delay time and Fermi velocity for parameters corresponding to semiconductors, where, for an effective mass $m^*=0.07m_e$, the energy difference of the main transition is around 1 eV and $t_0=0.06\times10^{-14}$ s, which leads to a Fermi velocity of around 10^9 cm/s and an electron density of 5.4×10^{13} cm^{-2}, which is somewhat higher than the typical carrier densities in semiconductor heterostructures.[15,16]

A particularly interesting case was the response to an infinitely large potential barrier along the minor axis applied at times $t\geq0$, starting from the same state as in the previous case (state 23). In Fig. 4(a), we see the evolution which is quite periodic with a frequency corresponding to the energy difference between the most relevant states involved (states 15, 16, 25, and 26 of the semiellipses, as shown in the approximate evolution where only these states were included). We, thus, observe here that due to the symmetry of the problem and the energy structure of the ellipse, only very few states take part and the time evolution becomes simple and robust.

If, on the other hand, we leave the barrier potential for a finite time t_1 only and then calculate the overlap of the original wave function to the remaining one after having removed the perturbation, we find another oscillatory behavior be-
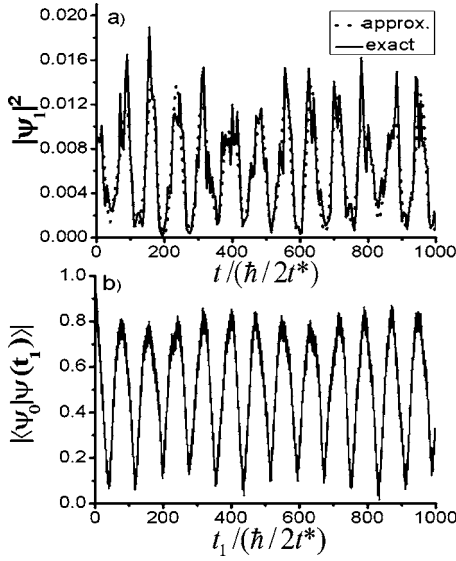
FIG. 4. (a) Time dependence of the probability density in focus 1 for an infinite potential barrier applied along the minor axis at time $t=0$. Solid and dot lines correspond to the time evolution of the exact and approximate wave functions, respectively. (b) Modulus of the overlap between the nonperturbed and final wave functions after the potential barrier had been applied during an interval t_1 and then removed (note the different parameters in the x axis used in both figures).

tween a nearly complete recovery of the original wave function and a nearly completely orthogonal state [see Fig. 4(b)].

III. INTERACTING CASE

In addition to the one-particle behavior studied in the previous section, we have analyzed the more interesting case of the effect of the focalizing properties of the ellipse on the interaction between two spins interacting via a superexchange term with the electron spins in the ellipse (Fig. 5). The Hamiltonian of the system reads

$$H = H_{el} + J(\vec{S}_1 \cdot \vec{\sigma}_1 + \vec{S}_2 \cdot \vec{\sigma}_2), \tag{1}$$

where

$$\vec{S}_i \cdot \vec{\sigma}_i = S_i^z \cdot \sigma_i^z + \frac{1}{2}(S_i^+ \cdot \sigma_i^- + S_i^- \cdot \sigma_i^+), \tag{2}$$

$\sigma_i^+ = c_{i\uparrow} c_{i\downarrow}$, and $\sigma_i^z = (n_{i\uparrow} - n_{i\downarrow})/2$, with $n_{i\sigma}$ the number operator and $c_{i\sigma}$ the destruction operator of an electron with spin σ in focus i of the ellipse. In the basis of eigenstates $|\alpha\rangle$ of the ellipse, these local operators can be expanded as $c_{i\sigma} = \Sigma_\alpha \Psi_{\alpha i} c_{\alpha\sigma}$, where $c_{\alpha\sigma}$ and $\Psi_{\alpha i}$ are the destruction operator and amplitude in state $|\alpha\rangle$. H_{el} is the Hamiltonian of the isolated ellipse with infinite walls described in Sec. II.

On this basis, the spin operators are expressed as

$$\sigma_i^z = \frac{1}{2} \sum_{\alpha_1 \alpha_2} \Psi_{\alpha_1 i}^* \Psi_{\alpha_2 i} (c_{\alpha_1 \uparrow}^\dagger c_{\alpha_2 \uparrow} - c_{\alpha_1 \downarrow}^\dagger c_{\alpha_2 \downarrow}),$$

$$\sigma_i^+ = \sum_{\alpha_1 \alpha_2} \Psi_{\alpha_1 i}^* \Psi_{\alpha_2 i} c_{\alpha_1 \uparrow}^\dagger c_{\alpha_2 \downarrow}. \tag{3}$$
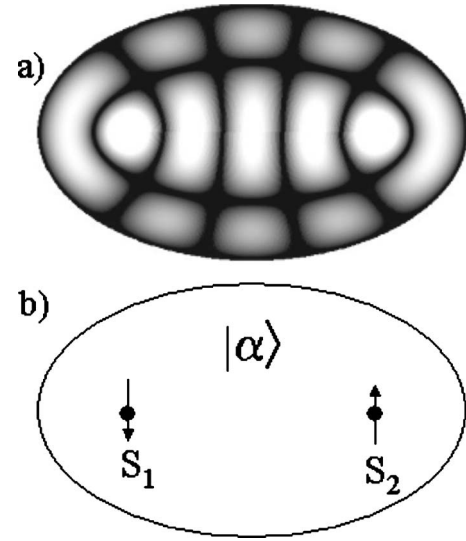

FIG. 5. (a) $|\psi_{23}|^2$ for the noninteracting ellipse with eccentricity $\epsilon=0.6$. White and black represent high and low electron densities, respectively. (b) Graphical representation of the system considered here, where $|\alpha\rangle$ represents an eigenstate of the nonperturbed ellipse. S_1 and S_2 are the impurity spins at the foci of the ellipse, which interact with the localized spins σ_i via a superexchange interaction J.

A. Static properties

We have solved this Hamiltonian numerically with exact diagonalization for a small number of levels and using the Lanczos technique for larger systems and different fillings corresponding to an even (closed shell) or odd (open shell) number of particles, N. The results for the spin gap Δ_s are depicted in Fig. 6, where we find a different behavior for even and odd numbers of electrons in the ellipse. For the former case, we observe a slow increase of the spin gap as a function of the interaction parameter J, which is quadratic and linear for small and large J, respectively. For an odd number of electrons, the behavior is linear from the beginning and the gap is somewhat larger than for the even filling. One can understand this behavior by using perturbation theory. For the even case (closed shell), the first correction to the energy stems from second-order nondegenerate terms, while for the odd filling (open shell), a first-order degenerate
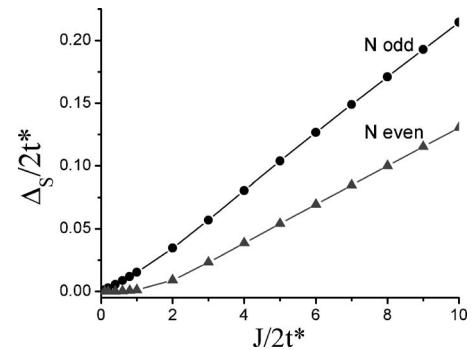

FIG. 6. Behavior of spin gap Δ_s with J for even (triangles) and odd (circles) numbers of electrons in the ellipse.
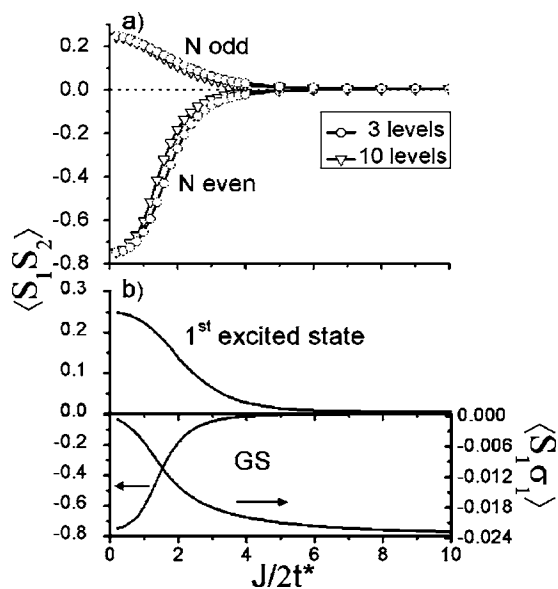
FIG. 7. (a) Spin-spin correlation between localized spins in the ground state for even and odd numbers of electrons and considering different numbers of levels in the ellipse. (b) Top panel: same as (a), N even, for the first excited state (having total spin $S=1$) showing the triplet character between the localized spins in both foci for small J. Lower panel: Correlation function between the localized spin S_1 and the spin of the itinerant electron σ_1 compared to the spin-spin correlation between localized spins for even N (for the ground state in all cases). For small J, the localized spins are entangled in a singlet state with no correlation with the electrons. For large J, these spins decouple while enhancing the local singlet interaction with the itinerant electron.

expansion is required, leading to a linear dependence.

For a realistic value[17] of the superexchange parameter for the Cu ellipse, $J_{exp}=0.1$ eV, we obtain $J/2t^* \simeq 0.05$ and a corresponding gap of around 10^{-5} eV $\simeq 0.12$ K for even filling, temperature under which the system is in a stable singlet state. For the semiconductor ellipse, the spin gap could be around ten times larger although we do not have any reliable estimation of J in this case. Thus, in both cases, copper or semiconducting corrals, this singlet state could be observed at sufficiently low temperatures.

One of the most important consequences of impurity spins in the presence of an elliptical corral like the one considered here is their enhanced correlation when situated at the foci of the system. For example, by analyzing the spin-spin correlation function in the ground state $\langle \psi_0 | \vec{S}_1 \vec{S}_2 | \psi_0 \rangle$, we find that they form a singlet or triplet for small J and even or odd particles, respectively [see Fig. 7(a)]. A ferromagnetic interaction between localized spins for odd numbers of electrons in the ellipse was also found in Ref. 7. For larger values of the interaction parameter, both impurity spins decorrelate. The results are weakly dependent on the number of levels considered, as also shown here.

It is also interesting to analyze the on-site correlation between the localized spin S_1 and the spin of the electron localized immediately above it, σ_1. In Fig. 7(b), we show how this interaction, which is antiferromagnetic, strengthens by increasing J, while S_1 decorrelates from S_2. In addition, as J
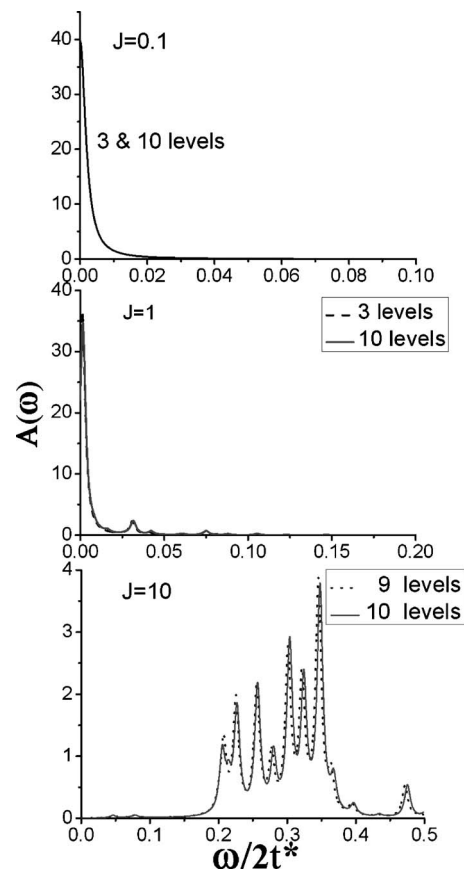

FIG. 8. Spin spectral function $A(\omega)$ for an even number of particles, three values of J, and different numbers of levels in the ellipse showing a negligible "finite size" effect. For small values of J, the spin gap is small and the first excitation is mainly a triplet state. See also Fig. 7(b), top panel.

increases, the electrons in the ellipse become more localized near the impurity in order to take advantage of the magnetic interaction forming a singlet with the localized spin in this limit.

B. Dynamical behavior

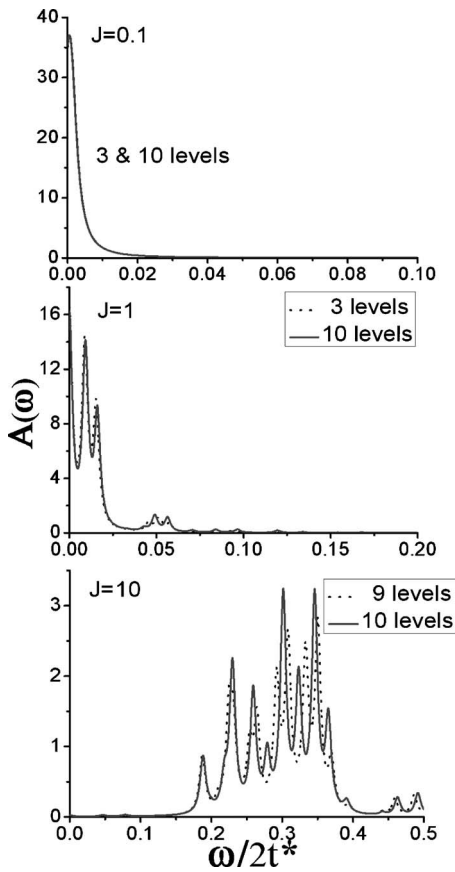We have calculated the spin response function to a spin excitation performed in focus 1,[18]

$$A(\omega) = -\frac{1}{\pi} \lim_{\eta \to 0^+} \text{Im } G(\omega + i\eta + E_0), \qquad (4)$$

where

$$G(z) = \langle \psi_0 | S_1^z (z-H)^{-1} S_1^z | \psi_0 \rangle. \qquad (5)$$

In Figs. 8 and 9, we show the results for different values of J and for even and odd fillings, respectively. For even N, we find that the excitations for small J consist mainly of one peak located at the spin gap, which is small. In this case, both localized spins form a very well defined singlet, whereas the first spin excitation has a triplet character, as can be seen in Figs. 7(b) top panel) and 10(a) (see below). For larger values of J, the spectral weight of this peak diminishes, other states get involved, and the spectral function is

FIG. 9. Same as Fig. 8 for odd N.

FIG. 10. Time dependence of the spin-spin correlation function between localized spins for the perturbed wave function $|\psi(t)\rangle = U(t)S_1^z|\psi_0\rangle$ for small and moderate interactions. For small J, the correlation is nearly a triplet as seen in previous figures.

more complicated [see also larger values of J in Fig. 7(b)]. For odd N and small J, both localized spins form a well defined triplet in the ground state and the first spin excitation corresponds to a spin flip of an electron spin, leaving S_1 and S_2 still entangled in a triplet state. In both cases, a negligible "size" dependence with the number of levels considered is found.

The fact that, for small J and an even number of particles, the first excitation is nearly purely a triplet can also be seen as a robust excitation which varies very slowly in time (see Fig. 10). Here, we depict $\langle \psi(t)|\vec{S}_1\vec{S}_2|\psi(t)\rangle$, where $|\psi(t)\rangle = U(t)S_1^z|\psi_0\rangle$, $U(t)$ is the time-evolution operator, and $|\psi_0\rangle$ is the interacting ground state. For $J=0.1$, we find a nearly constant behavior, scrumbling up with a larger amount of eigenstates for larger values of J. Note that the factor 1/4 which arises when comparing this correlation to a pure triplet behavior stems from the perturbation operator S_1^z applied to the ground state (the function $|\psi(t)\rangle$ is not normalized).

IV. CONCLUSIONS

We have studied static and dynamical properties of hard-wall elliptical quantum corrals subject to different kinds of perturbations. On one hand, we considered noninteracting systems and applied localized perturbation potentials in the foci and along the minor axis of the ellipse, finding robust osc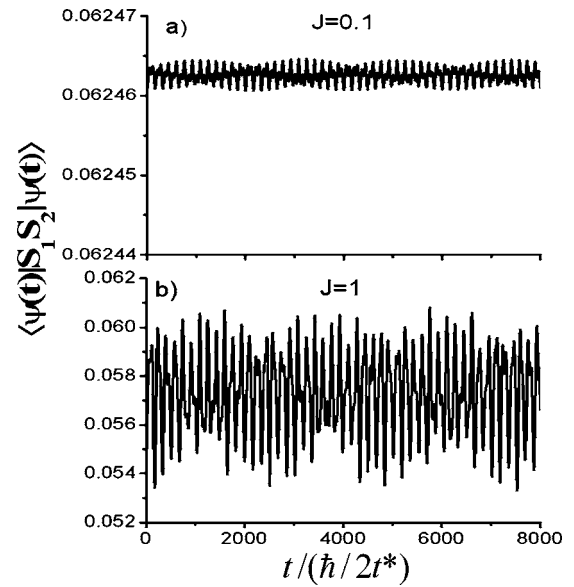illatory behaviors which are a consequence of the small amount of levels involved in the excitations. A finite time elapse was found in the case that the potential was applied to one focus until the perturbation reaches the unperturbed one. On the other hand, we studied the interacting case where two localized spins at the foci of the ellipse interacted antiferromagnetically with the itinerant electrons. In this case, we found a different behavior for even and odd electrons, which shows up in the spin gap and in the character of the ground state and the excitations. For the even particle number case and small interaction J, both localized spins are entangled in a (quasi-) singlet state, forming a (quasi-) triplet in the first excited state, which is the main spin excitation. These states are very robust, however, the spin gap is quadratically small with J. An interesting feature can be seen which resembles the Ruderman-Kittet-Kasuya-Yosida-Kondo-like transition occurring in the two-impurity system when increasing the Kondo interaction J: While the localized spins form a singlet state for small interaction, this coupling decreases for larger J, giving rise to an on-site singlet correlation between the spin and the itinerant electron.

In this work, we have shown that the focalizing properties of elliptic corrals lead to an interesting behavior between localized spins. For small J and even number of electrons in the ellipse, the system can be modeled by two spins interacting via an effective antiferromagnetic interaction parameter $H_{eff}=J_{eff}\vec{S}_1\cdot\vec{S}_2$, where $J_{eff}=\Delta_s$. For odd number of electrons, the interaction is ferromagnetic in the ground state. The character of this interaction can be controlled by changing the chemical potential of the system.

For small to moderate values of J ($J\lesssim 1$), the main results synthesized above still hold in the case of more realistic models of quantum ellipses, which include tunneling of the electrons in open corrals and inelastic processes with bulk electrons. In this parameter range, the broadening of the relevant energy levels is smaller than their separation.[10,13,19,20]

When larger interactions are included, higher levels which are more hybridized take part, and models including these processes should be considered.

[1] H. C. Manoharan, C. P. Lutz, and D. Eigler, Nature (London) **403**, 512 (2000).

[2] O. Agam and A. Schiller, Phys. Rev. Lett. **86**, 484 (2001).

[3] G. Chiappe and A. A. Aligia, Phys. Rev. B **66**, 075421 (2002); A. A. Aligia, *ibid.* **64**, 121102(R) (2001).

[4] M. Weissmann and H. Bonadeo, Physica E (Amsterdam) **10**, 44 (2001).

[5] D. Porras, J. Fernández-Rossier, and C. Tejedor, Phys. Rev. B **63**, 155406 (2001).

[6] G. A. Fiete, J. S. Hersch, E. J. Heller, H. C. Manoharan, C. P. Lutz, and D. M. Eigler, Phys. Rev. Lett. **86**, 2392 (2001).

[7] G. Chiappe and A. A. Aligia, Phys. Rev. B **66**, 075421 (2002).

[8] A. Lobos and A. A. Aligia, Phys. Rev. B **68**, 035411 (2003).

[9] K. Hallberg, A. A. Correa, and C. A. Balseiro, Phys. Rev. Lett. **88**, 066802 (2002).

[10] A. Correa, K. Hallberg, and C. Balseiro, Europhys. Lett. **58**, 6 (2002).

[11] V. S. Stepanyuk, L. Niebergall, W. Hergert, and P. Bruno, Phys. Rev. Lett. **94**, 187201 (2005).

[12] A. A. Aligia and A. M. Lobos, J. Phys.: Condens. Matter **17**, S1095 (2005).

[13] G. Fiete and E. Heller, Rev. Mod. Phys. **75**, 933 (2003).

[14] See http://cabtes55.cnea.gov.ar/tesisnizama/

[15] Y. W. Tan, J. Zhu, H. L. Stormer, L. N. Pfeiffer, K. W. Baldwin, and K. W. West, Phys. Rev. Lett. **94**, 016405 (2005).

[16] D. Ferry and S. Goodnick, *Transport in Nanostructures* (Cambridge University Press, Cambridge, 1997).

[17] W. Chen, T. Jamneala, V. Madhavan, and M. F. Crommie, Phys. Rev. B **60**, R8529 (1999).

[18] See, for example, G. Mahan, *Many-Particle Physics* (Plenum, New York, 1993).

[19] G. García-Calderón and L. Chaos-Cador, Phys. Rev. B **73**, 195405 (2006).

[20] S. Crampin, H. Jensen, J. Kröger, L. Limot, and R. Berndt, Phys. Rev. B **72**, 035443 (2005).